Proc. Annual Meeting of the Austrian Society for
Biomedical Engineering 2021 DOI: 10.3217/978-3-85125-826-4-17

A NEW CLASS OF ROBUST RF PULSES BY OPTIMAL CONTROL

C. Graf[1], M. Soellradl[1], C.S. Aigner[2], A. Rund[3], R. Stollberger[1]

[1]Institute of Medical Engineering, Graz University of Technology, Graz, Austria
[2]Physikalisch-Technische Bundesanstalt (PTB), Braunschweig and Berlin, Germany
[3]Institute of Mathematics and Scientific Computing, University of Graz, Graz, Austria

c.graf@tugraz.at

Abstract *— This work aimed to design and investigate inversion pulses that are robust among B_0 and B_1 inhomogeneities with a minimized pulse duration by optimal control. The optimized RF pulse was compared numerically to a state-of-the-art adiabatic RF pulse and a customized adiabatic one. All three RF pulses were investigated in extensive measurements on a 3T MRI system. Phantom measurements were performed to examine robustness with respect to B_0 and B_1. In vivo measurements of the knee emphasized the practicability of the proposed RF pulse which is shown to be robust among variations within B_0 and B_1.*

Keywords *— RF pulses, optimal control, robustness, B_0 inhomogeneities, B_1 inhomogeneities*

Introduction

Different MRI application experiments require inversion radio frequency pulses, i.e. pulses with a flip angle of 180°. However, for many applications, inhomogeneities within the B_0 and B_1 field are an issue, [1-9]. For special applications such as arterial spin labeling, even small deviations from the required exact inversion are unsatisfactory, [10]. Strong improvements regarding inversion efficiency could be achieved by using composite [6] or adiabatic [3] RF pulses, but at the cost of higher pulse energy and prolonged pulse duration. The design of RF pulses by optimal control has shown in the past that even conflicting requirements such as best pulse performance, short pulse duration, and limited pulse energy can be combined and fulfilled by using the entire parameter space [11-15]. This approach was already extended to account for B_0 and B_1 inhomogeneities, [4,16,17]. In [18], an ensemble-based optimal control formalism was used to include a time-minimal formalism and optimize for B_0 and B_1 robust inversion pulses. This work aims to compare the optimized RF pulse to state-of-the-art adiabatic RF pulses in phantom and in vivo measurements on a 3T MR system.

Theory and Methods

The goal of the optimization is to design RF pulses with robustness over a wide range of B_0 and B_1 variations, [18]. Therefore, we include B_1 scalings of 70% to 130% (i.e. a scale of the amplitude of the RF pulse by those factors) and B_0 offsets of +/-5ppm at 3T into the optimization. The optimization itself uses exact discrete derivatives supplied by adjoint calculus within a trust-region, semi-smooth quasi-Newton framework [13]. We use a 10ms RF pulse with random magnitude and random phase as initial. During optimization, the relaxation times were chosen to coincide with those of our cylindrical MR phantom (plastic bottle with diameter 14cm, length 42,5cm, filled with H_20 and contrast agent resulting in T_1=102ms, T_2=81ms at 3T). The underlying Bloch equations were solved using a symmetric operator splitting allowing for the inclusion of the relaxation effects, [19].

To compare the optimized pulse, two adiabatic, hyperbolic secant pulses are introduced. The first one (**HS1**) is commonly implemented for arterial spin labeling applications [10] and has a long pulse duration of 15.36ms. The second one (**HS2**) was designed so that the pulse duration and bandwidth coincide with those of the optimized pulse.

An extensive numerical comparison of all three RF pulses is performed including a broad set of B_0 offsets and B_1 scalings. The inversion efficiency is calculated for long a long repetition time (TR) with negligible T_1 influence for each pair of B_0 and B_1 as

$$eff = -\frac{I_{(inv)}}{I_0} = -\frac{S(x)\, M_{z(inv)}(x) \sin\alpha(x)}{S(x)\, M_0(x) \sin\alpha(x)} = -\frac{M_{z(inv)}(x)}{M_0(x)} \quad (1)$$

with M_z being the z-magnetization at the end of the respective RF pulse. Furthermore, M_0 is the initial magnetization and S(x) describes the signal intensity. For measurement, a slice selective excitation pulse with flip angle α is necessary. This excitation pulse is affected by RF inhomogeneities as well.

In addition, all three RF pulses were investigated in vivo measurements of the knee. We used the knee coil and we set the sequence parameters repetition time (TR) and echo time (TE) to TR=8000ms and TE=2.7ms. Those experiments were performed with a fixed B_1 scale of 100% and without additional B_0 offset. The flip angle was set to 90°.

CC BY

Published by Verlag der TU Graz
Graz University of Technology

DOI: 10.3217/978-3-85125-826-4-17

Results

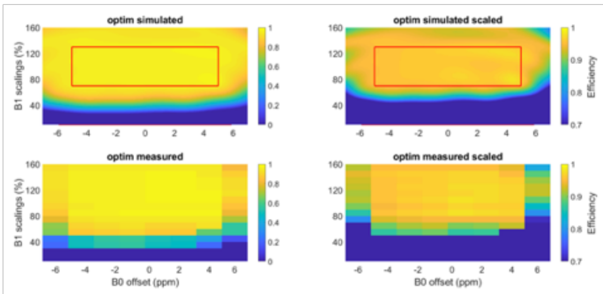

Figure 1: Simulated and measured inversion efficiencies of **optim** for B_1 scaled from 0% to 160% and ΔB_0 from -7ppm to 7ppm.

Figure 1 depicts the inversion efficiency of **optim** over a broad set of B_0 and B_1 variations. The red box indicates the area where the optimization was done (i.e. B_1 from 70% to 130% and B_0 from -5ppm to 5ppm). The pulse duration was reduced to T_p=3.25ms during optimization. The top figures show the numerical efficiencies which were calculated with the relaxation times of the phantom, while the bottom figures show the efficiencies measured on the MR scanner. The plots in the left column use an efficiency scale of 0% to 100% while in the right the plots are scaled from 70% to 100%. A very good inversion efficiency of more than 94.5% can be observed within the optimized area (red box). Furthermore, the figure shows strong accordance between numerical and measurement results.

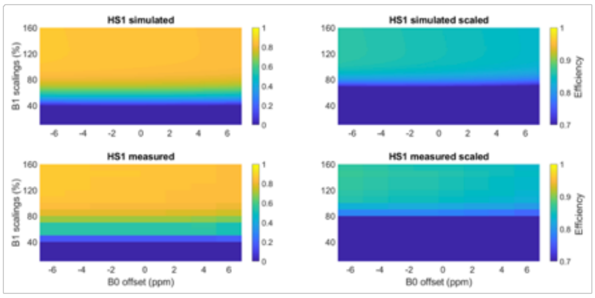

Figure 2: Simulated and measured inversion efficiencies of **HS1** for B_1 scaled from 0 % to 160% and ΔB_0 from -7ppm to 7ppm.

In Figures 2 and 3 we observe the inversion efficiencies of **HS1** and **HS2**. Again, a good accordance between simulated and measured inversion efficiencies can be observed. In both cases, the efficiency of **HS1** does not reach top values. There is strong robustness among changes within B_0, but for B_1 the efficiency is only acceptable for a scale of 100% and more. Below, the efficiency is less than 70%. In contrast, **HS2** shows a good inversion efficiency in the center of the plot (B_1 of 100% and B_0 at 0ppm). Only for a larger offset of B_0 the efficiency significantly decreases.

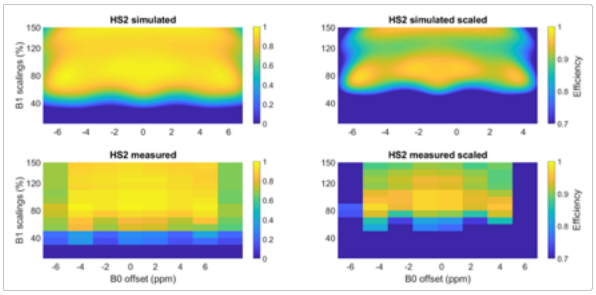

Figure 3: Simulated and measured inversion efficiencies of **HS2** for B_1 scaled from 0 % to 150% and ΔB_0 from -7ppm to 7ppm.

Figure 4 displays a sagittal cross-section of the knee using no pulse in the gradient echo sequence (top) and the **optim** inversion pulse (bottom). Figure 5 depicts the inversion profile measured with **optim**, a B_1-scale of 100% and without an additional B_0 offset. Between water and fat, bound protons at a resonance offset of 3.4ppm exist. Some chemical shift artifacts occur at tissue boundaries. We observe a severe decrease in signal intensity towards the proximal and distal parts in the image where the coil sensitivity and RF field strength drops to very low values. In Figure 5, the measured inversion efficiencies are depicted for all 3 RF pulses. Similarly to the phantom measurements, **optim** shows the best inversion efficiency among those 3 pulses within the defined field range. **HS1** has a decreased inversion efficiency even in the center of the knee with a fast loss in efficiency towards the coil edge. **HS2** shows a rather broad inversion capability, but with general lower inversion efficiency, in particular within the fatty bone marrow.

Discussion

During the optimization, the pulse duration of **optim** was reduced to 3.25ms, which is substantially shorter than the long duration of 15.36ms of **HS1**. **HS2** has the same pulse duration as **optim** by design. However, the maximum amplitude is increased by 25% which makes the pulse unsuitable for many applications due to the amplitude limitations of the MR scanner. Here, optimization for **optim** was started with random initialization. If existing for the application at hand, a sophisticated initialization is in general helpful for an optimizer, and also our optimizer can be used in this classical setup. However, optimizers that robustly converge from random initialization to a competitive minimizer, are rare, and open new perspectives (e.g. finding new – possibly better - local minimizers or even quasi-global optimization by multi-random initialization).

CC BY

Published by Verlag der TU Graz
Graz University of Technology

DOI: 10.3217/978-3-85125-826-4-17

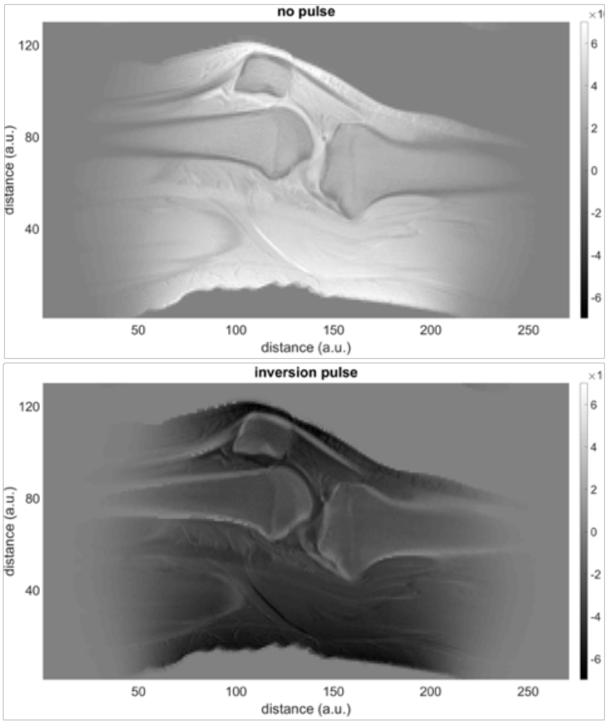

Figure 4: Sagittal cross-section of the knee. The top picture displays the image without an inversion pulse ($S(\mathbf{x}) \cdot M_0(\mathbf{x}) \cdot \sin\alpha(\mathbf{x})$), the bottom picture with an inversion pulse ($S(\mathbf{x}) \cdot M_{z(inv)}(\mathbf{x}) \cdot \sin\alpha(\mathbf{x})$) using **optim**. The inhomogeneous signal intensity represents the inhomogeneous RF field and coil sensitivity of the knee coil.

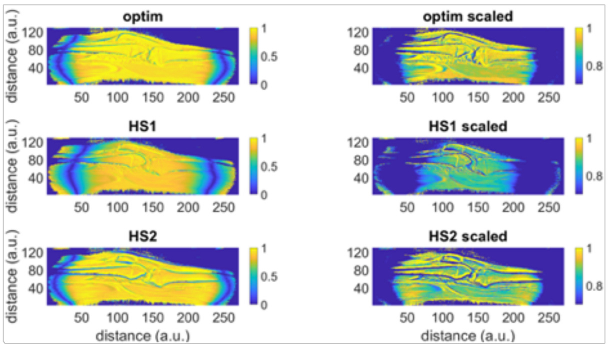

Figure 5: Inversion efficiencies for measurements of the knee. **Optim** (left), **HS1** (middle) and **HS2** (bottom). Efficiency scale of 0% to 100% (left) and 70% to 100% (right).

Figure 5 displayed the comparison of the three inversion pulses for in vivo applications. Similar to the phantom results, **optim** showed the best behaviour in terms of inversion efficiency. The long adiabatic pulse **HS1** showed already in simulation and phantom measurement only a moderate inversion efficiency which was validated in the in vivo measurement. One reason for that is its rather long pulse duration which results in relaxation effects affecting the efficiency. The short adiabatic pulse **HS2** could underline its behaviour in the in vivo experiments yielding a good efficiency. However, the main drawback is the higher amplitude required. Furthermore, in Figure 5, we depict line artifacts due to chemical shift behaviour.

A consequent future improvement of this work would be to jointly control the slice-selective gradient for slice-selective applications. Furthermore, an extension to optimize for excitation pulses, i.e. RF pulses with a flip angle less than 180° would be desired.

Conclusion

Inversion pulses were optimized within an optimal control framework with the aim of B_0- and B_1-robustness and a reduced pulse duration. The numerical and measured comparison to state-of-the-art adiabatic pulses revealed a significant improvement in terms of inversion efficiency while being short and fulfilling all physical limitations.

References

[1] Wang, J., Mao, W. et al.: *Factors influencing flip angle mapping in MRI: Pulse shape, slice-select gradients, off-resonance excitation and B0 inhomogeneities*, Magn Reson Med 2006;56:463-468.
[2] de Graaf, R.A.: *In Vivo NMR Spectroscopy*, John Wiley & Sons, 2007.
[3] Bernstein, M.A., King, K.F. et al.: *Handbook of MRI Pulse Sequences*, Elsevier Academic Press, 2004.
[4] Kobzar, K., Skinner, T.E. et al.: *Exploring the limits of broadband excitation and inversion: II. RF-power optimized pulses.* J Magn Reson 2008;194:58-66.
[5] Hurley, A.C., Al-Radaideh, A. et al.: *Tailored RF pulse for magnetization inversion at ultrahigh field*, Magn Reson Med 2010;63:51-58.
[6] Moore J., Jankiewicz, M. et al.: *Composite RF pulses for B_1^+-insensitive volume excitation at 7 Tesla*, J Magn Reson 2010;205:50-62.
[7] Warnking, J.M., Pike, G.B.: *Bandwidth-modulated adiabatic RF pulses for uniform selective saturation and inversion,* Magn Reson Med 2004;52:1190-1199.
[8] Alsop, D.C., Detre, J.A. et *al.*: *Recommended Implementation of Arterial Spin-Labeled Perfusion MRI for Clinical Applications: A Consensus of the ISMRM Perfusion Study Group and the European Consortium for ASL in Dementia*, Magn Reson Med 2014.
[9] Wang, K., Shao, X. et al.: *Optimization of adiabatic pulses for pulsed arterial spin labeling at 7 Tesla: Comparison with pseudo-continuous arterial spin labeling,* Magn Reson Med 2021;6:3277-3240.
[10] Garcia, D.M., Duhamel, G. et al.: *Efficiency of Inversion Pulses for Background Suppressed Arterial Spin Labeling,* Magn Reson Med 2005;54:366-372.

CC BY

DOI: 10.3217/978-3-85125-826-4-17

[11] Conolly, S., Nishimura, D. et al.: *Optimal control solutions to the magnetic resonance selective excitation problem,* IEEE Trans Med Imaging 1986;5:106-115.

[12] Aigner, C.S., Clason, C. et al.: *Efficient high-resolution RF pulse design applied to simultaneous-multislice excitation*, J Magn Reson 2016;263:33-44.

[13] Rund, A., Aigner, C.S. et al.: *Magnetic Resonance RF Pulse Design by Optimal Control with Physical Constraints*, IEEE Trans Med Imaging 2018;37:461-472.

[14] Rund, A., Aigner, C.S. et al.: *Simultaneous multislice refocusing via time optimal control,* Magn Reson Med 2018;80:1416-1428.

[15] Aigner, C.S., Rund, A. et al.: *Time optimal control-based RF pulse design under gradient imperfections*, Magn Reson Med 2020;2:561-574.

[16] van Reeth, E., Ratiney, H. et al.: *Optimal control design of preparation pulses for contrast preparation in MRI,* J Magn Reson 2017;279:39-50.

[17] Graf, C., Aigner, C.S. et al.: *Inversion pulses with B1-robustness and reduced energy by optimal control,* In Proceedings of the ISMRM, 2020.

[18] Graf, C., Soellradl, M. et al.: *Time optimal control based design of robust inversion pulses,* In Proceedings of the ISMRM, 2021.

[19] Graf, C., Rund, A. et al.: *Accuracy and performance analysis for Bloch and Bloch-McConnell simulation methods,* J Magn Reson, 2021.

CC BY